

Mode Decomposition in Three Dimensional Cracks using Mutual Integrals

Young Jong Kim*

* Mechanical Engineering, Sangju National University, Kyungbuk, South Korea

ABSTRACT

A numerical scheme is proposed to obtain the individual stress intensity factors in an axisymmetric crack and in a three dimensional mixed mode crack. The method is based on the path independence of J and M integral and mutual or two-state conservation integral, which involves two elastic fields. Some numerical example are presented to investigate the effectiveness and applicability of the method for an axisymmetric crack and a three dimensional penny shaped crack problem under mixed mode.

Keywords : Stress intensity factor, conservation integral, mixed mode crack, three dimensional penny shaped crack

1. Introduction

Conservation integrals in elasticity have been widely applied to the fracture mechanics, among which the J integral is the most popular one. The J integral is path-independent and has been shown to be identical to Irwin's energy release rate associated with the collinear extension of a crack in an elastic solid[15]. It has been related to the crack tip stress intensity factors in both linear and nonlinear elastic solids subjected to infinitesimal deformations[6]. It is necessary to evaluate the individual stress intensity factors separately for mixed mode crack problems in order to investigate the crack growth and the crack propagation. However, the evaluation of the J integral alone does not determine the individual stress intensity factors, K_I , K_{II} and K_{III} separately.

Many works on mixed mode crack problems using the path-independent integrals have been reported. Bui[2] developed a technique using the J integrals associated with Mode I and Mode II, in which the symmetric and antisymmetric parts of the planar displacement, strain and stress fields about the crack plane are separated. Stern et al.[17] employed another conservation integral based on Betti's reciprocal work theorem with known auxiliary fields. Later the method

was extended for the straight interfacial cracks by Hong and Stern[5]. For planar cracks, Yau et al.[20], Wang and Yau[18], Matos et al.[12] and Shih and Asaro[16] utilized a new class of conservation integral known as mutual integral or two-state conservation integral, proposed by Chen and Shield[3]. Choi and Earmme[4] employed the two-state L-integral to evaluate stress intensity factors in circular arc-shaped interfacial crack. Recently Im and Kim[8] showed that the two-state M-integral is applicable for computing the intensity of the singular near-tip field for a generic isotropic composite wedge including planar cracks. The main interest of fracture mechanics is shifting from two to three dimensional crack problems and particularly it becomes increasingly important to study three dimensional mixed mode crack problems for the crack growth and the crack propagation prediction.

This study presents a method to obtain the individual stress intensity factors in case of axisymmetric and three dimensional cracks in mixed mode using J and the associated two-state integral. The method is based on the path-independence of J and two-state J integral which involves two independent elastic fields, from which each stress intensity factor may be evaluated from the displacements and stresses remote from the crack tip. In the next section the basic formulation for the method are described and the solution procedure is established. The

implementation of the method is explained in Section 3 In Section 4 numerical examples are carried out in order to demonstrate the usefulness of the method.

2. Formulation of the problems

2.1 Axisymmetric formulation

In three dimensional infinitesimal deformations of homogeneous isotropic bodies, M-integral is defined as [9]

$$M = \int_{\Gamma} \left(Wx_i n_i - T_j u_i x_j - \frac{1}{2} T_i u_i \right) dA \quad (i = 1, 2, 3) \quad (1)$$

where W is the strain energy density, u_i the displacement, n_i the unit outward normal vector, and T_i is the traction vector.

Consider crack problems in an elastic, homogeneous, isotropic axisymmetric solid under axisymmetric loading conditions. As a result of its axisymmetry, equation (1) can then be rewritten as [10]

$$M = 2\pi \int_{\Gamma} \left(Wx_\alpha u_\alpha - T_\alpha u_{\alpha,\beta} x_\beta - \frac{1}{2} T_\alpha u_\alpha \right) x_i ds \quad (2)$$

where the subscript α, β indicate the components in the r-z or the x_1 - x_2 plane (see Fig. 2), and Γ encloses the crack tip. Note that x_1 and x_2 are used for r and z whenever it is convenient to do so. Physically, equation (2) implies that M-integral is a driving force for a crack to expand uniformly[1].

Straightforward argument reveals that the M integral has the following relationships for the axisymmetric cracks[10] in the absence of mode III or torsion.

$$J_I = \frac{M_I}{2\pi r_c^2} = \alpha K_I^2, \quad J_{II} = \frac{M_{II}}{2\pi r_c^2} = \alpha K_{II}^2, \quad J = J_I + J_{II} \quad (3)$$

where $\alpha = \frac{1-\nu^2}{E}$ (E : Young's modulus, ν : Poisson's ratio), and r_c is the r or the x_1 coordinate of the crack tip, that is, the shortest distance from the z-axis to the crack tip.

It should be noted here that the J integral in equation (3) alone does not provide adequate information for determining the individual stress intensity factors K_I and K_{II} in a mixed mode crack problem. Following Chen and Shield[3], we consider two independent elastic states of a penny shaped crack: the target problem field denoted by superscript (1) and the auxiliary field denoted by (2). Let the elastic state from the superposition of the two elastic fields be denoted by superscript (0). Then the J integral for the resulting state has the following form:

$$J^{(0)} = J^{(1)} + J^{(2)} + J^{(1,2)} \quad (4)$$

in which $J^{(1)}$, $J^{(2)}$ and $J^{(1,2)}$ are given as

$$J^{(l)} = \frac{1}{r_c^2} \int_{\Gamma} F_m^{(l)} n_m x_i ds, \quad (l = 1, 2) \quad (5a)$$

with $F_m^{(1)} = W^{(1)} x_i \delta_{im} - \sigma_{ik}^{(1)} u_{i,j}^{(1)} x_j \delta_{km} - \frac{1}{2} \sigma_{in}^{(1)} u_i^{(1)} \delta_{nm}$

$$J^{(1,2)} = \frac{1}{r_c^2} \int_{\Gamma} F_m^{(1,2)} n_m x_i ds \quad (5b)$$

with

$$F_m^{(1,2)} = W^{(1,2)} x_i \delta_{im} - \left(\sigma_{ik}^{(1)} u_{i,j}^{(2)} + \sigma_{ik}^{(2)} u_{i,j}^{(1)} \right) x_j \delta_{km} - \frac{1}{2} \left(\sigma_{in}^{(1)} u_n^{(2)} + \sigma_{in}^{(2)} u_n^{(1)} \right) \delta_{im}$$

where δ_{ij} is the Kronecker delta and $W^{(1,2)}$ is the mutual strain energy density of the elastic body, defined by

$$W^{(1,2)} = C_{ijkl} u_{i,j}^{(1)} u_{k,l}^{(2)} = C_{ijkl} u_{i,j}^{(2)} u_{k,l}^{(1)} \quad (6)$$

In equations (5a,b), $\sigma_{ij}^{(1)}$ and $u_i^{(1)}$ can be obtained from analytic or numerical solution to the target problem field along a properly selected integration path Γ , while $\sigma_{ij}^{(2)}$ and $u_i^{(2)}$ are given from an auxiliary field, which is chosen in a convenient manner.

Recalling the relationships of equation (3), one finds that the J integral for the state (0) may be expressed as

$$J^{(0)} = \alpha \left\{ \left[K_I^{(1)} + K_I^{(2)} \right]^2 + \left[K_{II}^{(1)} + K_{II}^{(2)} \right]^2 \right\} \quad (7)$$

which leads to

$$J^{(0)} = J^{(1)} + J^{(2)} + 2\alpha \left(K_I^{(1)} K_I^{(2)} + K_{II}^{(1)} K_{II}^{(2)} \right) \quad (8)$$

Comparison between equations (4) and (8) reveals that

$$J^{(1,2)} = 2\alpha \left(K_I^{(1)} K_I^{(2)} + K_{II}^{(1)} K_{II}^{(2)} \right) \quad (9)$$

The J integral shown in equations (5b) and (9) deals with the interaction term only and is to be used for solving mixed mode penny shaped crack problems in a linear elastic solid. It should be noted here that the $J^{(1,2)}$ integral(mutual integral) is related to the details of the stresses and deformation at the crack tip (i.e., K_I and K_{II} in equation (9)) Due to the path-independence of this integral, however, yet may be evaluated in the region away from the crack tip (i.e., the integral in equation (5b)), where such a calculation can be carried out with greater accuracy and convenience than near the crack tip.

Equation (5b) together with equation (9) provides, in fact, sufficient information for determining the stress intensity factors for a mixed mode fracture problem of a penny shaped crack, when proper known auxiliary field solutions are introduced. Let the superscript "(2a)" indicate the solution for an auxiliary elastic field, wherein the body under consideration is in the state of

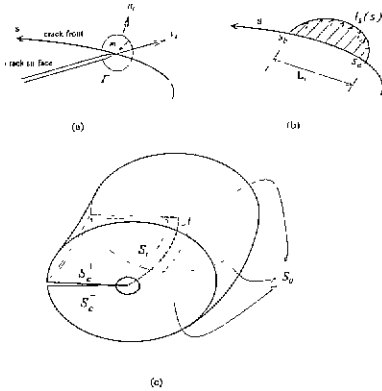


Fig. 1(a) Conventions at curvilinear crack front.

Fig. 1(b) Virtual crack advance between S_a and S_b

Fig. 1(c) Inner tubular surface S_i and outer arbitrary surface S_o .

mode I deformation only, i.e.,

$$K_I^{(2a)} \neq 0 \text{ and } K_{II}^{(2a)} = 0 \tag{10}$$

Equation (9) can be simplified as

$$J^{(1,2a)} = 2\alpha K_I^{(1)} K_I^{(2a)} \tag{11}$$

For the target problem field and for the auxiliary field of Mode I, we have, respectively:

$$J^{(1)} = \alpha \left\{ [K_I^{(1)}]^2 + [K_{II}^{(1)}]^2 \right\}, \quad J^{(2a)} = \alpha [K_I^{(2a)}]^2 \tag{12}$$

Equations (11) and (12) leads to the expressions of the individual stress intensity factors for the target field in terms of the conservation integrals, $J^{(1)}$, $J^{(2a)}$ and $J^{(1,2a)}$:

$$K_I^{(1)} = \sqrt{\frac{J^{(1,2a)}}{4\alpha J^{(2a)}}}, \quad K_{II}^{(1)} = \sqrt{\frac{1}{\alpha} \left[J^{(1)} - \frac{[J^{(1,2a)}]^2}{4J^{(2a)}} \right]} \tag{13}$$

It should be noted that the integrals $J^{(1)}$, $J^{(2a)}$ and $J^{(1,2a)}$ have to be calculated accurately for a proper evaluation of $K_I^{(1)}$ and $K_{II}^{(1)}$. For a given crack geometry and loading condition, this can be achieved by integrating equations (5a,b) along a properly selected band in the far field utilizing the domain integral expression [11, 14].

2.2 Three dimensional formulation

In three dimensional infinitesimal deformation of homogeneous isotropic elastic bodies the J integral is given as [9]

$$J_k = \int_{\Gamma} (Wn_k - T_i u_{i,k}) dA \tag{14}$$

where A indicates a closed surface. Note that the pointwise value of J along the crack front is required for mode decomposition. According to Moran and Shih [13], $J(s)$ is given as

$$J(s) = \frac{-\lim_{r \rightarrow 0} \int_{S_r} l_k H_{ij} m_j d\Gamma}{\int_{L_c} l_k v_k ds} \tag{15}$$

where “s” denotes the coordinate along the crack front of a three dimensional crack; $H_{ij} = W\delta_{ij} - \sigma_y u_{i,k}$, l_k , which is short for $l_k(s)$, indicates the component of crack advance vector; v_k , which is short for $v_k(s)$, represents an outward unit vector normal to crack front on the crack plane and m_j is the normal to Γ pointing towards the crack front. i.e. $m_j = -n_j$ on Γ as shown in Fig. 1a. Furthermore, S_r is an inner tubular surface and L_c is a small interval on the line of the crack front for virtual crack extension.

As the crack tip is approached in a three dimensional crack, asymptotically the plain strain state prevails [15] and therefore we can use the following relationships for the three dimensional mixed mode crack

$$J_I = \alpha K_I^2, \quad J_{II} = \alpha K_{II}^2, \quad J_{III} = \frac{\alpha}{1-\nu} K_{III}^2, \tag{16}$$

$$J = J_I + J_{II} + J_{III}$$

where $\alpha = \frac{1-\nu^2}{E}$ (E : Young's modulus, ν : Poisson's ratio)

As in the axisymmetric case, the J integral in equations (15) and (16) alone does not provide adequate information for determining the individual stress intensity factors K_I , K_{II} and K_{III} in a mixed mode crack problem. Another information may be obtained from the two-state J-integral [3]. Consider two independent elastic states of a penny shaped crack in an elastic medium, each denoted by superscript (1) and (2). Let the equilibrium state from the superposition of the two states be denoted by superscript (0). Then the J integral for the superimposed state is obtained in the following form:

$$J^{(0)} = J^{(1)} + J^{(2)} + J^{(1,2)} \tag{17}$$

in which $J^{(k)} (k = 1, 2)$ is defined by equation (15), $J^{(1,2)}$ is given as

$$J^{(1,2)} = -\lim_{r \rightarrow 0} \int_{\Gamma(r)} l_k H_{ij}^{(1,2)} m_j d\Gamma / \int_{L_c} l_k v_k ds \tag{18}$$

with $H_{ij}^{(1,2)} = W^{(1,2)} \delta_{ij} - (\sigma_y^{(1)} u_{i,k}^{(2)} + \sigma_y^{(2)} u_{i,k}^{(1)})$

From equation (16), one finds that the J integral for the elastic state (0) may be written as

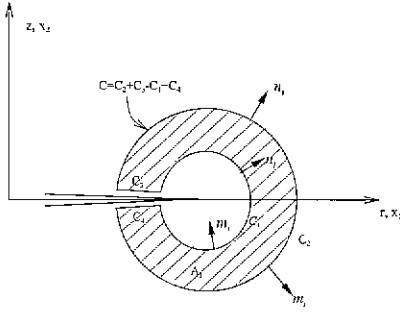


Fig. 2 Simply connected region A_I enclosed by the contour C on the crosssection of an axisymmetric crack

$$J^{(0)} = J^{(1)} + J^{(2)} + 2\alpha \left(K_I^{(1)} K_I^{(2)} + K_{II}^{(1)} K_{II}^{(2)} + \frac{I}{I-\nu} K_{III}^{(1)} K_{III}^{(2)} \right) \quad (19)$$

and comparison to equation (17) yields

$$J^{(1,2)} = 2\alpha \left(K_I^{(1)} K_I^{(2)} + K_{II}^{(1)} K_{II}^{(2)} + \frac{I}{I-\nu} K_{III}^{(1)} K_{III}^{(2)} \right) \quad (20)$$

Equation (18) together with equation (20) provides, in fact, sufficient information for determining the individual stress intensity factors for a mixed mode fracture problem when two known auxiliary solutions are introduced. Let two auxiliary solutions be denoted by a superscript (2a) and (2b). The auxiliary state (2a) is chosen to be a pure mode I state, and (2b) to be a pure mode III. Then $J^{(2a)}$ and $J^{(2b)}$ are written as

$$J_I^{(2a)} = \alpha [K_I^{(2a)}]^2, \quad J_{III}^{(2b)} = \alpha \frac{I}{I-\nu} [K_{III}^{(2b)}]^2 \quad (21)$$

Together with equations (16) and (20), these leads to the following expression for $K_I^{(1)}$, $K_{II}^{(1)}$ and $K_{III}^{(1)}$ in terms of $J^{(1)}$, $J^{(1,2a)}$, $J^{(2a)}$, $J^{(1,2b)}$ and $J^{(2b)}$

$$K_I^{(1)} = \frac{J_I^{(1,2a)}}{\sqrt{4\alpha J_I^{(2a)}}}, \quad \text{and} \quad J_I^{(1)} = \frac{[J_I^{(1,2a)}]^2}{4J_I^{(2a)}} \quad (22)$$

$$K_{III}^{(1)} = \sqrt{\frac{E}{I+\nu}} \frac{J_{III}^{(1,2b)}}{\sqrt{4J_{III}^{(2b)}}}, \quad \text{and} \quad J_{III}^{(1)} = \frac{[J_{III}^{(1,2b)}]^2}{4J_{III}^{(2b)}} \quad (23)$$

$$K_{II}^{(1)} = \frac{I}{\sqrt{\alpha}} \sqrt{J^{(1)} - \frac{[J_I^{(1,2a)}]^2}{4J_I^{(2a)}} - \frac{[J_{III}^{(1,2b)}]^2}{4J_{III}^{(2b)}}}, \quad \text{and} \quad J_{II}^{(1)} = \alpha [K_{II}^{(1)}]^2 \quad (24)$$

Note that the path-independent integrals on the right hand side of the above expressions may be calculated accurately, transforming equation (18) into the domain integral expression [11, 14], as will be shown in the next section.

3. Finite Element Implementation

3.1 Axisymmetric finite element implementation

In the foregoing we have established the mode decomposition method for axisymmetric and three dimensional cracks under mixed mode. Accuracy of the method described in Section 2 depends on how accurately the conservation integrals are evaluated. The integration path may be chosen along the elements boundaries or through the Gaussian points. Li et al.[11], Nikishkov and Atluli[14] and Shih and Asaro[16] have introduced appropriate weighting functions to obtain area/domain representation of the J integral. They have concluded that a very accurate value of J is obtained using the domain representation and the value of J so obtained is insensitive to the types of weighting function. In an analogous manner it is possible to recast the line integral J of equations (5) into the area integral:

$$J = \frac{I}{r_c^2} \int_{A_I} F_m x_r \frac{\partial q}{\partial x_m} dA \quad (25)$$

where A_I is an area enclosed by Γ as shown in Fig. 2 and the function F_m is given in equations (5a,b). Moreover, q is a weight function which has the value of zero on the contour Γ and one on the inner contour. Use is made of the equilibrium equation and divergence theorem in deriving the expression (25).

3.2 Three dimensional finite element implementation

The values of J(s) and the two-state integral along a three dimensional crack front are given by the limiting contour integral as seen in equations (15) and (18). Following Moran and Shih[13], we can show that the domain integral representation is obtained as

$$J(s) = \frac{- \int_{V_c} H_{kj} q_{k,l} dV}{\int_{L_c} l_k(s) v_k(s) ds} \quad (26)$$

where " L_c " is the crack front line from S_a to S_b (see Fig. 1b); the weight function " q_k " is smooth enough for the indicated operations to be carried out and is defined as follows

$$q_k = \begin{cases} l_k & \text{on } S_l \\ 0 & \text{on } S_0 \\ \text{orthogonal to } m_i & \text{on } S_c^+ \text{ and } S_c^- \\ \text{otherwise arbitrary.} & \end{cases} \quad (27)$$

where S_l, S_0, S_c^+, S_c^- and m_i are indicated in Fig. 1.

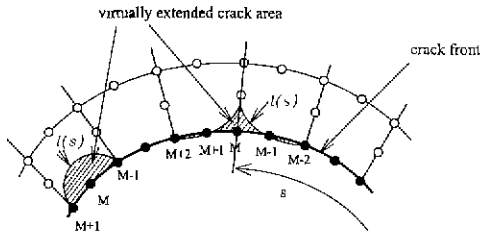


Fig. 3 Local advance of the crack front for 20-node 3D element

In a three dimensional analysis the virtual crack extension has to be applied to a single node point on the crack front for evaluating the local value of the energy release rate. For the 20-node three-dimensional isoparametric element, a new crack front is defined by the quadratic interpolation function as shown in Fig. 3. The volume V is identified with the collection of elements which contain the line L_c . Thus, in the finite element framework, for considering the increase in cracked area due to the shift of a given particular node M we take L_c to be the line connecting the nodes $M-1$, M and $M+1$ for mid nodes and the nodes $M-2$, $M-1$, M , $M+1$ and $M+2$ for corner nodes as shown in Fig. 3. Then, the local crack front advance is therefore taken as follows [11]

$$l = \sum_{k=1}^{20} N^k Q^k \quad (28)$$

where N^k is the triquadratic shape function and Q^k is the nodal values for the k -th node. Note that $Q^k = 0$ if the k -th node is on S_0 . For nodes inside V , Q^k is given by interpolation between the nodal values on L_c and S_0 .

4. Numerical examples and discussion

The procedures just outlined have been programmed for studying an axisymmetric penny shaped crack and a three dimensional penny shaped crack under mixed mode in isotropic solids. The numerical calculations for mixed mode crack problems are carried out with the finite element code ABAQUS[22]. This code supplies the required displacements and stresses at the Gaussian points to a separate program developed for evaluating J -integral and two-state conservation integrals.

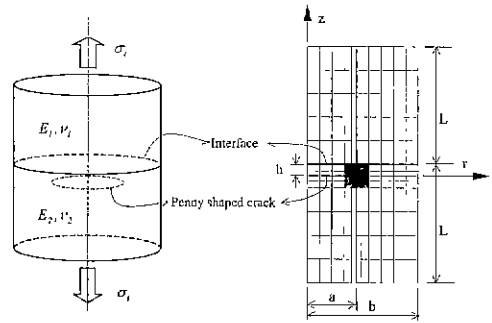


Fig. 4(a) Axisymmetric subinterface penny shaped crack.

Fig. 4(b) Finite element model for axisymmetric subinterface penny shaped crack.

4.1 Axisymmetric sub-interface penny shaped crack

To illustrate the decomposition method for axisymmetric mixed mode cracks, an axisymmetric sub-interface penny shaped crack is selected as an example problem. The problem of a straight crack paralleling an interface between two dissimilar materials has attracted a substantial amount of attention due to its potential application in various kinds of bonding problems [7, 19].

In this paper the problem of a penny shaped crack paralleling an interface between two dissimilar materials under tension is investigated. The loading condition and the crack geometry under investigation are shown in Fig. 4a ($\sigma_t = 6.895 \times 10^5 \text{ N/m}^2$). The cylinder has a radius $b = 0.0572 \text{ m}$; total length of $2L = 0.127 \text{ m}$. The penny shaped crack has a radius $a = 0.0254 \text{ m}$ ($a/b = 0.444$); a distance from the interface to the penny shaped crack is $h = 0.00635 \text{ m}$. Each material is taken to be isotropic and elastic. The upper part of the cylinder has elastic properties of $E_1 = 2.069 \times 10^9 \text{ N/m}^2$ and $\nu_1 = 0.3$. The lower part containing a penny shaped crack has elastic properties of $E_2 = 2.069 \times 10^{11} \text{ N/m}^2$ and $\nu_2 = 0.3$.

To examine the accuracy and the convergence of the results, a typical finite element mesh for a penny shaped crack paralleling an interface between two dissimilar materials is selected as shown in Fig. 4b wherein a total of 298 eight noded isoparametric axisymmetric elements are used. To find a Mode I auxiliary field, we consider a body of the same geometry as in the target problem, but composed of the lower material ($E = E_2$ and $\nu = \nu_2$)

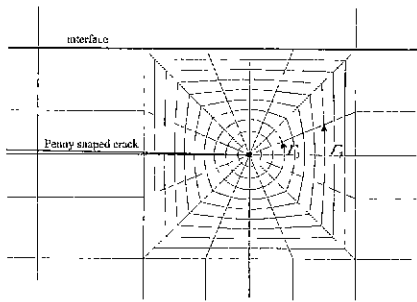


Fig. 5 The detailed element arrangement around the crack tip and The paths of the integration domains 3 and 7 are indicated.

only. Because the body is made of a homogeneous material, it will undergo a pure Mode I deformation under a remote tension $\sigma_1 = 6.895 \times 10^5 \text{ N/m}^2$. Note that the foregoing mode decomposition scheme is applicable only when an auxiliary field is found for the target problem, i.e. the geometry and the material properties should coincide between the auxiliary field and the target problem. Hence we restrict our attention to the lower part of the target field, which has the same geometry and properties as the auxiliary field. This is equivalent to removing the upper part and applying the external traction, which is acting upon the lower material by the upper one, so that the mode decomposition scheme is now applied on the lower part of the body. It is under a mixed mode in the target problem while it is under pure Mode I in the auxiliary field. The first integration domain is comprised of 16 elements adjoining the crack tip; the second domain has the next 16 elements adjoining the first integration domain. In this manner, the integration domains 3 through 9 are continued. The detailed element arrangement around the crack tip and the domain selected for integration are given in Fig. 5 wherein the paths of the integration domains 3 and 7 are indicated. The calculations for J-integrals are carried out according to the domain integral (25) in a separate post-processing program, and the two-state integrals are calculated in the same manner.

The path independence of J and two-state integral has been checked numerically by using different domains of integration.

The values of J and two-state integral as calculated by the discrete domain formula of the type of equation

Table 1 Axisymmetric Analysis Result for a penny shaped crack

Domain	$J^{(1)}$	$J^{(2)}$	$J^{(3)}$	K_I	K_{II}
	(Pa-m)				
1	4.0466E-01	3.2799E-01	7.6300E-02	2.8305E+02	1.0892E+02
2	4.1197E-01	3.3347E-01	7.7558E-02	2.8544E+02	1.1032E+02
3	4.1235E-01	3.3307E-01	7.7640E-02	2.8496E+02	1.1194E+02
4	4.1240E-01	3.3312E-01	7.7645E-02	2.8499E+02	1.1191E+02
5	4.1242E-01	3.3314E-01	7.7645E-02	2.8501E+02	1.1189E+02
6	4.1244E-01	3.3316E-01	7.7643E-02	2.8502E+02	1.1188E+02
7	4.1246E-01	3.3316E-01	7.7643E-02	2.8502E+02	1.1188E+02
8	4.1246E-01	3.3316E-01	7.7643E-02	2.8502E+02	1.1189E+02
9	4.1244E-01	3.3316E-01	7.7642E-02	2.8502E+02	1.1187E+02
Average excluding the first domain					
	4.1237E-01	3.3317E-01	7.7642E-02	2.8496E+02	1.1170E+02

(25) for the various domains are listed in Table 1. We observe that the variation in the computed J and two-state integral from one domain to another is within 1 percent excluding the near tip domain of the first domain. Effects of E_1/E_2 are examined by taking various material constant E_1 's or E_1/E_2 's for the given lower part containing a penny shaped crack and $\nu_1 = \nu_2 = 0.3$. A plot of the variation of the computed K_I and K_{II} with the increase of E_1/E_2 is shown in Fig. 6. This shows well the mixed mode of the sub-interface penny shaped crack even under uniaxial tension loading, because K_I and K_{II} are of the same order of magnitude. It is noticed that K_I is always higher than K_{II} in the entire range of E_1/E_2 examined. In the case of $E_1/E_2 < 1$, K_I and K_{II} increase as E_1/E_2 decreases. K_I and K_{II} remain relatively unchanged with E_1/E_2 greater than 30. Note that K_{II} disappears $E_1/E_2 = 1$. This K_I is found to be $K_I = 1.2089 \sigma_1 \sqrt{a}$, and this is well

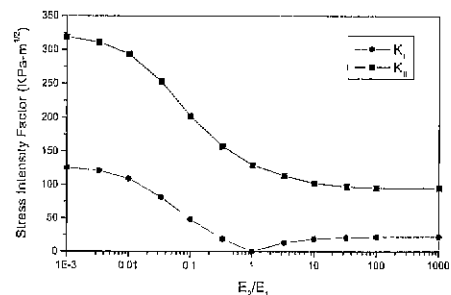


Fig. 6 The variation of K_I and K_{II} with the increase of E_1/E_2 ($\nu_1 = \nu_2 = 0.3$)

compared with $K_I = 1.1903 \sigma_r \sqrt{a}$ for an axisymmetric crack in a homogeneous body from Benthem and Koiter[21], with the difference being only 1.56 %.

4.2 Three dimensional penny shaped crack under nonaxisymmetric loading

Because no published reference solution is available yet, to examine the accuracy and the convergence of the decomposition method for a three dimensional mixed mode crack we first compare the results from the decomposition method for three dimensional mixed mode cracks with those for the axisymmetric mixed mode crack in the previous section. We consider the full three dimensional model consisting of a 360° revolution of the same axisymmetric model as in the previous section about the z axis. The model is discretized with ten elements along the circumference in a 180° segment. The typical finite element mesh for the full three dimensional model is similar to that illustrated in Fig. 7.

A total of 5740 twenty noded isoparametric elements are used. The elements adjoining the crack front are set to possess the inverse square root singularity at the corner nodes on the crack tip by choosing the mid nodes to be located on the quarter point.

We briefly discuss the setting up of the integration domains for calculating J and two-state integrals associated with a unit virtual advance of a finite crack front segment (e.g. see Fig.7). The first integration domain is comprised of a collection of elements adjoining the crack front: the domain consists of two layers of elements in the circumferential direction, amounting to a total of 32 elements, for a unit virtual advance of a corner node while it contains only one layers of elements or a total of 16 elements if a unit

virtual advance is imposed on a mid node. The second domain is obtained by adding one ring of elements around the first domain; thus the second domain has a total of 64 elements for a virtual advance of a corner node and a total of 32 elements for a virtual advance of a mid node. In this manner, the integration domains 3 through 9 are continued

The variation of q_k and in particular the nodal values Q within the integration domain are generated in the following manner. First we prescribe q_3 to be zero everywhere since the normal to the crack front is in the radial direction on the X-Y plane as shown in Fig. 7b. Next q_1 and q_2 are defined to be $q \cos \theta$ and $q \sin \theta$ respectively.

The loading condition and the crack geometry under investigation are the same as those in the previous section. ($E_1 = 2.069 \times 10^9 \text{ N/m}^2$, $E_2 = 2.069 \times 10^{11} \text{ N/m}^2$ and $\nu_1 = \nu_2 = 0.3$) As an auxiliary solution, Mode I loading condition was used for the cylinder of a homogeneous material $E_1 = E_2 = 2.069 \times 10^{11} \text{ N/m}^2$.

Table 2 Three dimensional analysis result for a penny shaped crack under nonaxisymmetric loading

Corner Node					
Domain	$J^{(1)}$	$J^{(1,2)}$	$J^{(2)}$	K_I	K_{II}
	(Pa-m)			(KPa-m ^{1/2})	
1	4.2172E-01	3.4032E-01	7.9547E-02	2.8765E-02	1.1455E-02
2	4.1729E-01	3.3676E-01	7.8715E-02	2.8613E+02	1.1393E-02
3	4.1624E-01	3.3592E-01	7.8521E-02	2.8578E+02	1.1379E+02
4	4.1584E-01	3.3559E-01	7.8441E-02	2.8564E+02	1.1374E+02
5	4.1559E-01	3.3540E-01	7.8398E-02	2.8549E+02	1.1368E+02
6	4.1542E-01	3.3526E-01	7.8369E-02	2.8549E+02	1.1368E+02
7	4.1531E-01	3.3517E-01	7.8347E-02	2.8546E+02	1.1366E+02
8	4.1522E-01	3.3512E-01	7.8332E-02	2.8544E+02	1.1364E+02
9	4.1514E-01	3.3506E-01	7.8321E-02	2.8542E+02	1.1359E+02
Average excluding the first domain					
	4.1575E-01	3.3554E-01	7.8432E-02	2.8562E+02	1.1371E+02
Mid Node					
Domain	$J^{(1)}$	$J^{(1,2)}$	$J^{(2)}$	K_I	K_{II}
	(Pa-m)			(KPa-m ^{1/2})	
1	4.1673E-01	3.3631E-01	7.8610E-02	2.8594E+02	1.1385E+02
2	4.1230E-01	3.3274E-01	7.7777E-02	2.8442E+02	1.1324E+02
3	4.1125E-01	3.3189E-01	7.7580E-02	2.8407E+02	1.1311E+02
4	4.1083E-01	3.3156E-01	7.7502E-02	2.8391E+02	1.1305E+02
5	4.1058E-01	3.3135E-01	7.7454E-02	2.8382E+02	1.1301E+02
6	4.1042E-01	3.3123E-01	7.7425E-02	2.8377E+02	1.1299E+02
7	4.1030E-01	3.3114E-01	7.7404E-02	2.8374E+02	1.1297E+02
8	4.1021E-01	3.3107E-01	7.7388E-02	2.8371E+02	1.1294E+02
9	4.1015E-01	3.3104E-01	7.7377E-02	2.8369E+02	1.1290E+02
Average excluding the first domain					
	4.1076E-01	3.3151E-01	7.7488E-02	2.8389E+02	1.1302E+02

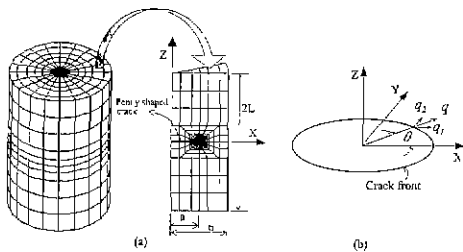


Fig. 7(a) Three dimensional finite element model for penny shaped crack under nonaxisymmetric loading

Fig. 7(b) q definition at node M.

Table 3 Comparison between the axisymmetric analysis result and the three dimensional analysis result

	$J^{(0)}$	$J^{(I)}$	$J^{(II)}$	K_I	K_{II}
	(Pa-m)			(KPa-m ^{3/2})	
Axisymmetric analysis					
Average	4.1237E-01	3.3317E-01	7.7642E-02	2.8496E-02	1.1170E+02
Three dimensional analysis					
Corner Node	4.1575E-01	3.3554E-01	7.8432E-02	2.8562E+02	1.1371E+02
Mid Node	4.1076E-01	3.3151E-01	7.7488E-02	2.8389E+02	1.1302E+02
Average	4.1326E-01	3.3352E-01	7.7960E-02	2.8476E+02	1.1337E+02
Max. relative difference from axisymmetric analysis result*					
	0.8	0.5	1.0	0.4	1.8

$$* \frac{\max |a - b|}{a} \times 100$$

a : axisymmetric analysis result
 b : three dimensional analysis result
 (corner node or mid node result)

The results from the present decomposition method for three dimensional mixed mode crack are shown in Table 2. It is seen from these tables that J-integrals and two-state integral are path independent except the first domain. In Table 3, they are compared with the results from the axisymmetric analysis of the foregoing section. Comparison of the results shows that the three dimensional solution is in an excellent agreement with the axisymmetric solution. In the three dimensional solutions the J and two-state integrals for a virtual advance of a corner node differ only slightly from those for a virtual advance of a mid node.

To illustrate the mode separation for three dimensional mixed mode cracks, selected is an example of an circular cylinder containing a penny-shaped crack at its center under nonaxisymmetric loading. The crack geometry and the finite element mesh are shown in Fig 7. The cylinder has a radius $b=0.0508$ m; total length of $2L=0.152$ m. The penny shaped crack has a radius $a=0.0254$ m ($a/b=0.5$). For auxiliary solutions, two different loadings are chosen; one is a uniform tension, generating a pure mode I deformation, and the other a torsion, giving rise to a pure mode III.

To apply nonaxisymmetric loading, the lower end face of the circular cylinder at $z=-L$ is constrained against motion in the x, y and z, whereas the uniform displacement boundary condition of $u_x = 2.54 \times 10^{-6}$ m and $u_z = 7.62 \times 10^{-8}$ m are applied on the other end face of the circular cylinder at $z=L$.

The solution procedure starts from the choice of the

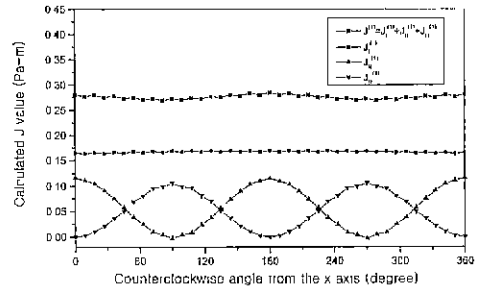


Fig. 8 The calculated pointwise values of $J_I^{(I)}$, $J_{II}^{(I)}$, $J_I^{(II)}$ and $J_{II}^{(II)}$ along the crack front of the penny shaped crack

independent auxiliary fields, which are obtained by the choice of the two different loadings – uniform tension and torsion. For the auxiliary field of Mode I, the same finite element model as that for the target field are used under tension with $\sigma_t = 6.895 \times 10^5$ N/m² and for the auxiliary field of mode III under torsion load with the applied torque of 4.61 kg-m. With both of the auxiliary field data and the target field data from ABAQUS output file the evaluation of the J and two-state integral is carried out for domain selected as described in the case of the axisymmetric case in this section.

A plot of the variation of the computed $J_I^{(I)}$, $J_{II}^{(I)}$, $J_I^{(II)}$ and $J_{II}^{(II)}$ along the crack front of the penny shaped crack is shown in Fig. 8. In the plot, $J_I^{(I)}$ at the intersection of the crack boundary with the x axis is slightly greater than that at the intersection of the crack boundary with the y axis. $J_{II}^{(I)}$ is constant along the crack front of the penny shaped crack as is expected. Note that $J_I^{(II)}$ and $J_{II}^{(II)}$ vary like the curves for each of the squares of $\cos \theta$ and $\sin \theta$ along the crack front of the penny shaped crack. It is noticed that $J_I^{(II)}$ is greatest at the intersection of the crack boundary with the x axis and vanishes at the intersection of the crack boundary with the y axis. On the other hand, $J_{II}^{(II)}$ vanishes at the intersection of the crack boundary with the x axis and is greatest at the intersection of the crack boundary with the y axis. This is consistent with the applied displacements of u_x and u_z on the top face of the cylinder.

With these J and two-state integrals, K_I , K_{II} and K_{III} are obtained from equations (22), (23) and (24). A plot of the variation of the computed K_I , K_{II} and K_{III} along the crack front is shown in Fig. 9. Note that

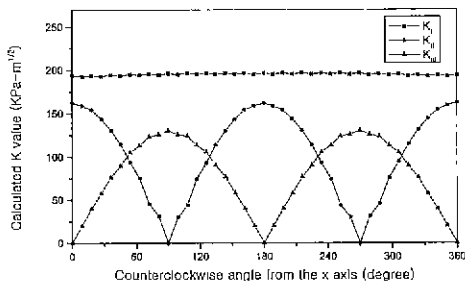


Fig. 9 The variation of the computed K_I , K_{II} and K_{III} along the crack front of the penny shaped crack

K_I is constant along the crack front of the penny shaped crack. As expected, K_{II} and K_{III} vary like curves of $\cos\theta$ and $\sin\theta$ respectively along the crack front of the penny shaped crack. Each of the stress intensity factors K_I , K_{II} and K_{III} have the variation consistent with that of each of $J_I^{(1)}$, $J_{II}^{(1)}$ and $J_{III}^{(1)}$ along the circumferential direction. The key to success of this mode decomposition scheme is the choice of appropriate auxiliary solutions with their stress intensity factors known. It turns out to be very successful for axisymmetric cracks under nonaxisymmetric loadings. It is quite straightforward to pick up suitable auxiliary solutions, which are given as pure Mode I and Mode III solutions. However, the choice are not straightforward for a generic three dimensional crack with no axisymmetry in geometry, and yet to be answered in the future.

5. Conclusions

A method of analysis, based on the conservation laws of elasticity and the fundamental relationships in fracture mechanics, has been proposed for studying axisymmetric mixed mode crack and three dimensional mixed mode crack problems. The method is based on the path-independence of J-integral and two-state integral. Path-independence of the J and two-state integrals enables us to compute the individual stress intensity factors accurately and effectively from the domain integral expression. The solution procedure has been established and shown to be computationally efficient and operationally simple, involving only the choice of appropriate auxiliary solutions and the calculation of the J and two-state integrals with the aid of the domain

integral expression. However, the choice of appropriate auxiliary solutions is yet to be answered for a generic three dimensional crack.

References

1. Budiansky, B., and Rice, J. R. "Conservation Laws and Energy Release Rate," J. Appl. Mech. 40, pp. 201-203, 1973.
2. Bui, H. D. "Associated Path Independent J Integrals for Separating Mixed Modes," J. Mech. Phys. Solids Vol. 31, pp. 439-448, 1983.
3. Chen, F. H. K., and Shield, R. T. "Conservation Laws in Elasticity of the J Integral Type," J. Appl. Math. Phys.(ZAMP) 28, pp. 1-22, 1977.
4. Choi, N.Y., and Earmme, Y.Y. "Evaluation of Stress Intensity Factors in Circular Arc-shaped Interfacial Crack using L Integral," Mechanics of Materials 12, pp. 141-153, 1992.
5. Hong, C. C., and Stern, M. "The Computation of Stress Intensity Factors in Dissimilar Materials," J. Elast. Vol. 8, pp. 21. 1978.
6. Hutchinson, J.W. "Singular Behavior at the End of a Tensile Crack in a Hardening Material," J. Mech. Phys. Solids Vol. 16, pp. 13-31, 1968.
7. Hutchinson, J.W., Mear, M. E., and Rice, J. R. "Crack Paralleling an Interface Between Dissimilar Materials," J. Appl. Mech. 54, pp. 828-832, 1987.
8. Im, S., and Kim, K.S. "Application of the Two-state M Integral for Computing an Intensity Factor of a Singular Near-tip Field for a Generic Composite Wedge," J. Mech Phys. Solids (in print)
9. Knowles, J. K., and Sternberg, E. "On a Class of Conservation Laws in Linearized and Finite Elastostatics," Arch. Rat. Mech. Anal. 44, pp. 187. 1972.
10. Kuo, A. "On the Use of a Path-independent Line Integral for Axisymmetric Cracks with Nonaxisymmetric Loading." J. Appl. Mech. 54, pp. 833-837, 1987.
11. Li, F.Z., Shih, C.F., and Needleman, A. "A Comparison of Methods for Calculating Energy Release Rates," Eng. Fracture Mechanics, Vol. 21 pp. 405-421, 1985.
12. Matos, P. P. L., McMeeking, R.M., P.G. Charalambides, P.G., and Drory, M.D. "A Method for

- Calculating Energy Release Rates." *Eng. Fract. Mech. Anal.* 44, pp. 405, 1985.
13. Moran, B., and Shih, C.F. "Crack Tip and Associated Domain Integrals from Momentum and Energy Balance." *Eng. Fracture Mechanics*. Vol. 27 pp. 615-642, 1987.
 14. Nikishkov, G. P. and Atluh, S. N. "An equivalent domain integral method for computing crack tip integral parameters in nonelastic, thermo-mechanical fracture," *Eng. Fracture Mechanics*. Vol. 26 pp. 851-867, 1987.
 15. Rice, J.R. "A Path-independent Integral and Approximate Analysis of Strain Concentrations by Notches and Cracks," *ASME J. Appl Mech.* 35, pp. 379-386, 1968.
 16. Shih, C. F., and Asaro, R. J. "Elastic-Plastic Analysis of Cracks on Bimaterial Interfaces: Part II-Structure of Small-Scale Yielding Fields," *J. Appl. Mech.* 55, pp. 299-316, 1988.
 17. Stern, M., Becker, E. B., and Dunham, R. S. "A Contour Integral Computation of Mixed Mode Stress Intensity Factors," *Int. J. Fracture*, Vol. 12, pp. 359-368, 1976.
 18. Wang, S. S., and Yau, J. F. "Interfacial Cracks in Adhesively Bonded Scarf Joints," *AIAA J.* 19, pp. 1350-1356, 1981.
 19. Yang, M., and Kim, K. "The Behavior of Subinterface cracks with Crack-face Contact," *Eng. Fracture Mechanics*. Vol. 44, pp. 155-165, 1993.
 20. Yau, J. F., Wang, S. S., and Corten, H. T. "A Mixed Mode Crack Analysis of Isotropic Solids using Conservation Laws of Elasticity," *J. Appl. Mech.* 47, pp. 335-341, 1980.
 21. Benthem, J.P. and Koiter, W.T. *Asymptotic Approximations to Crack Problems, Method Analysis and Solutions of Crack Problems*, G.C. Sih, ed., Noordhoff International Publishing, Holland, 1973
 22. Hibbit, H.D. Karlsson, B. and Sorenson, E.P. *ABAQUS User's Manual*, Hibbit, Karlsson and Sorenson Inc., Providence, RI, 1997.